JOURNAL OF GUIDANCE, CONTROL, AND DYNAMICS
Vol. 27, No. 4, July–August 2004

Optimization of Variable-Specific-Impulse Interplanetary Trajectories

Lorenzo Casalino* and Guido Colasurdo†
Politecnico di Torino, 10129 Torino, Italy

An indirect optimization method is used to find optimal trajectories that use solar electric propulsion. Missions that exploit variable specific impulse are compared to constant-specific-impulse trajectories, and the benefit, in terms of payload, is highlighted. The presence of limits on the attainable values of the specific impulse and the use of dual-mode thrusters, which operate only at two discrete values of specific impulse, are also considered. The analytical formulation of the problem is presented, and the necessary conditions for an optimal solution are discussed. Numerical examples deal with planet rendezvous missions; a Mercury mission would largely benefit from the management of the available power, which exhibits a tenfold variation caused by the vehicle's varying distance from the sun. The optimization method can also deal with planetary gravity assists; Mercury missions, which exploit Venus flybys, are optimized and their characteristics discussed. Results show that the dual-mode thrusters provide almost the same propellant savings as the more complex variable-specific-impulse thrusters.

Introduction

ELECTRIC propulsion will likely be the preferred option for solar-system exploration in the near future; the higher specific impulse, compared to chemical propulsion, reduces the propellant requirements and increases the payload. Ion thrusters seem to be suitable for this kind of missions; the success of the Deep Space 1 mission, which has completed more than 14,000 h of thrusting, testifies to the reliability of electrostatic thrusters.[1]

The power of the electric thruster is proportional to the specific impulse I_{sp} and to the thrust level, if the thruster efficiency is assumed to be constant. A high I_{sp} reduces the propellant requirement, whereas a high thrust level reduces the trip time. When a constant-I_{sp} operation is considered, the mission designer selects the specific impulse to obtain the best compromise between mission payload and trip time. Optimization methods are used to search for minimum-propellant trajectories. An increasing number of revolutions around the main body reduces the propellant consumption, and a time constraint is necessary to make the optimization problem meaningful. In this case, the mission designer is able to obtain the optimal value of the specific impulse to accomplish the trajectory in the assigned time, once the available power is given. The power level, which maximizes the payload, can also be determined when the specific mass of the electric source is assigned.

Variable-I_{sp} ion thrusters will probably be available soon,[2,3] and other classes of electric thrusters with a variable specific impulse, namely Hall thrusters[4] and Vasimr thrusters,[5] are currently under development. A thruster that can exploit a wide range of values of the specific impulse could be used both for escape from Earth and for the interplanetary portion of the flight. However, a smaller range of operational I_{sp} is also useful to improve performance, as it allows better management of the available power during the interplanetary trajectory. General considerations[6,7] suggest increasing I_{sp} as the propellant is gradually consumed; the optimal value of the instantaneous specific impulse is inversely proportional to the spacecraft mass in the absence of gravitational losses. However, the control law is modified by the presence of this kind of loss; I_{sp} is reduced when the spacecraft is in positions where a large thrust level is advisable (for instance, at the apsides of the orbit), whereas it is increased when the thrust cannot be usefully exploited (for instance, when the constant-I_{sp} trajectory has a coast arc). In particular, the thrust acceleration must be proportional to the magnitude[8,9] of the primer vector,[10] which can be considered as an index of the usefulness of thrusting. An engine with unbounded variable I_{sp} is always kept on and the specific impulse continuously varied. A time constraint is required, also in this case, to avoid a meaningless solution with very high specific impulse and an infinite trip time. Coast arcs again appear when the constraint is applied to the thrust-on time instead of applying the constraint to the overall mission time.[11]

The purpose of the present paper is to quantify the benefit that is obtained using a solar electric propulsion system, which includes a variable-I_{sp} thruster. Most of the benefit can however be obtained without the requirement of variable I_{sp}; a thruster, which can provide only two different values of I_{sp} (dual-mode or dual-I_{sp} thruster), performs almost as well as the variable-I_{sp} thruster. The analysis is carried out by investigating the best strategy to reach Mars, Venus, and Mercury. The optimal control laws are derived and discussed. A procedure that determines the optimal values of the specific impulse, which must be provided by the constant-I_{sp} and dual-I_{sp} thrusters, is presented. Simpler boundary conditions than those used in actual missions are assumed to avoid the influence of the phase angle between the planets on the performance, thus maintaining a general significance of the results. In fact, a nonfavorable phase angle depletes the maximum payload and modifies the desired characteristics of the propulsion system, in particular in the constant-I_{sp} case. More complex boundary conditions, including the treatment of the gravity assist, can be found elsewhere.[11–13] The same papers also present the technique that can be adopted to determine the optimal value of the available power at 1 AU, that is, the optimal area of the solar-array surface.

Equations of Motion

A point-mass spacecraft with variable mass m is considered. The patched conic approximation is adopted, and the time spent inside the planets' spheres of influence is neglected; therefore, the equations of motion are integrated only in the heliocentric reference frame.[11] The state equations are

$$\frac{\mathrm{d}\boldsymbol{r}}{\mathrm{d}t} = \boldsymbol{v} \tag{1}$$

Presented as Paper 2002-4897 at the AAS/AIAA Astrodynamics Specialist Conference, Monterey, CA, 5–8 August 2002; received 28 January 2003; revision received 25 June 2003; accepted for publication 11 November 2003.

*Associate Professor, Dipartimento di Energetica, Corso Duca degli Abruzzi, 24. Member AIAA.

†Professor, Dipartimento di Energetica, Corso Duca degli Abruzzi, 24. Associate Fellow AIAA.

$$\frac{\mathrm{d}\boldsymbol{v}}{\mathrm{d}t} = \boldsymbol{g} + \frac{\boldsymbol{T}}{m} \tag{2}$$

$$\frac{\mathrm{d}m}{\mathrm{d}t} = -\frac{T}{c} \tag{3}$$

where $\boldsymbol{r}$ and $\boldsymbol{v}$ are the spacecraft position and velocity vectors, $\boldsymbol{g}$ is the solar gravitational acceleration (an inverse-square gravity field is assumed throughout), $\boldsymbol{T}$ is the engine thrust, $c = g_0 I_{\mathrm{sp}}$ is the exhaust velocity, which is proportional to the specific impulse, via the acceleration g_0 caused by the Earth's gravity at the planet's surface. Variables are normalized using the radius of Earth's orbit, its corresponding circular velocity, and the initial mass of the spacecraft as reference values. The period of Earth's orbit is 2π, and the reference time unit is therefore 58.132 days. The thruster employs solar electric propulsion, and the solar radiation power is in an inverse-square relation with the distance from the sun. Accordingly, the available power is $P_a = P_1/r^2$ for missions to Venus and Mars, where P_1 is the nominal available power at 1 AU and r is expressed in nondimensional units. The spacecraft approaches the sun closely during a Mercury mission, and it might be necessary to reduce the exposed surface of the solar panels to avoid extreme thermal loads; the relation[14] $P_a = r^{-1.6}[1 - 2.8945(1-r)^4]P_1$ is used in this case.

Boundary Conditions

The spacecraft leaves the Earth's sphere of influence on a parabola, that is, with zero hyperbolic excess velocity. The procedure could however provide the optimal value of the hyperbolic excess velocity once the characteristics of the chemical engine, which is used to escape from the Earth, are assigned.[12,13] The boundary conditions at the initial point (subscript 0) are

$$\boldsymbol{r}_0 = \boldsymbol{r}_E(t_0) \tag{4}$$

$$\boldsymbol{v}_0 = \boldsymbol{v}_E(t_0) \tag{5}$$

$$m_0 = 1 \tag{6}$$

where subscript E denotes the Earth.

The arrival at the target planet with zero hyperbolic excess velocity is also considered, as it appears to be the most general condition for the rendezvous, before the characteristics of the engine for the orbit insertion or an alternative braking technique are specified. The imposed boundary conditions at the final point (subscript f) are therefore

$$\boldsymbol{r}_f = \boldsymbol{r}_T(t_f) \tag{7}$$

$$\boldsymbol{v}_f = \boldsymbol{v}_T(t_f) \tag{8}$$

where subscript T denotes the target planet. The payload is the performance index that is maximized. The mission can be performed with lower thrust and, conversely, with larger specific impulse as the trip time is increased, thus improving the payload. Therefore, a constraint on the trip time $\tau = t_f - t_0$ is imposed. In the presence of a planetary flyby, the relevant boundary conditions are enforced.[11]

Trajectory Optimization

The trajectory is controlled by the thrust magnitude and direction. The desired thrust level

$$T = 2\eta(P/c) \tag{9}$$

is obtained by selecting the exhaust velocity and the engine input power P (constant thruster efficiency η is assumed throughout), taking the operational constraints into account. The input power is always limited by the availability of solar power ($P \le P_a$); the exhaust velocity can be bounded ($c_{\min} \le c \le c_{\max}$), or, in the limiting case, constant.

An adjoint variable is associated to each state equation, and the Hamiltonian is defined as

$$H = \boldsymbol{\lambda}_r^T \boldsymbol{v} + \boldsymbol{\lambda}_v^T(\boldsymbol{g} + \boldsymbol{T}/m) - \lambda_m(T/c) \tag{10}$$

According to Pontryagin's maximum principle (PMP), the optimal controls maximize the Hamiltonian. The thrust must be parallel to the primer vector ($\boldsymbol{\lambda}_v^T \boldsymbol{T} = \lambda_v T$) and, using also Eq. (9), the Hamiltonian is rewritten as

$$H = \boldsymbol{\lambda}_r^T \boldsymbol{v} + \boldsymbol{\lambda}_v^T \boldsymbol{g} + (\lambda_v/m - \lambda_m/c)2\eta(P/c) \tag{11}$$

where only

$$H' = (\lambda_v/m - \lambda_m/c)2\eta(P/c) \tag{12}$$

contains the control variables. The theory of optimal control provides the Euler–Lagrange equations for the adjoint variables

$$\frac{\mathrm{d}\boldsymbol{\lambda}_r^T}{\mathrm{d}t} = -\boldsymbol{\lambda}_v^T \left[\frac{\partial \boldsymbol{g}}{\partial \boldsymbol{r}}\right] - \left(\frac{\lambda_v}{m} - \frac{\lambda_m}{c}\right)\frac{2\eta}{c}\frac{\partial P}{\partial \boldsymbol{r}} \tag{13}$$

$$\frac{\mathrm{d}\boldsymbol{\lambda}_v^T}{\mathrm{d}t} = -\boldsymbol{\lambda}_r^T \tag{14}$$

$$\frac{\mathrm{d}\lambda_m}{\mathrm{d}t} = \frac{\lambda_v}{m^2}2\eta\frac{P}{c} = \frac{\lambda_v}{m^2}T \tag{15}$$

The state, adjoint, and control variables in Eq. (12) are always positive. (This is obvious for P, c, m, and λ_v, which is the magnitude of the primer vector; $\lambda_m < 0$ has never been found in the present work.) The Hamiltonian linearly depends on P via Eq. (12); a bang-bang control is therefore optimal for the power level. Singular arcs are excluded; they are usually absent outside the atmosphere, and their necessity would be shown by incongruities in the results.[15]

Constant-I_{sp} Thruster

During a constant-I_{sp} operation ($c = c_{\min} = c_{\max}$), the input power, or, equivalently, the thrust, is the only control. Equation (12) is usually rewritten as

$$H' = (\lambda_v/m - \lambda_m/c)T = S_F T \tag{16}$$

and the sign of the switching function S_F determines when the thruster is turned on or off. The maximum available power (i.e., maximum thrust level) is adopted when $S_F > 0$, whereas the engine is switched off when $S_F < 0$ to maximize H', according to PMP. The optimal constant value of c for a given P_1 is also computed and used in the present work. For this purpose, c is no longer considered as a control, but as an additional state variable, which is constant along the trajectory ($\mathrm{d}c/\mathrm{d}t = 0$). An adjoint variable λ_c is added, and the differential equation

$$\frac{\mathrm{d}\lambda_c}{\mathrm{d}t} = -\frac{2\eta P}{c^2}\left(\frac{\lambda_v}{m} - 2\frac{\lambda_m}{c}\right) \tag{17}$$

is integrated, while the boundary conditions for optimality require $\lambda_{c0} = \lambda_{cf} = 0$. The optimal value of c always grows as the trip time is increased, improving the payload; c would grow to infinity if the constraint on the trip time were removed.

Variable-I_{sp} Thruster

If the exhaust velocity is no longer constant, c and P are the control variables. $H' = 0$ is obtained by switching the engine off, but, according to PMP, the thruster is usefully switched on, and H' becomes positive, if at least one admissible value of c, which makes S_F positive, exists. The entire available power $P = P_a$ is therefore used when the power switching function

$$S_P = \lambda_v/m - \lambda_m/c_{\max} \tag{18}$$

which contains the maximum admissible value of c, is positive, but the thruster is switched off when $S_P < 0$. One soon deduces that continuous operation at maximum power level is necessary if no upper limit for the exhaust velocity is present ($c_{\max} = \infty$, and S_P is always positive).

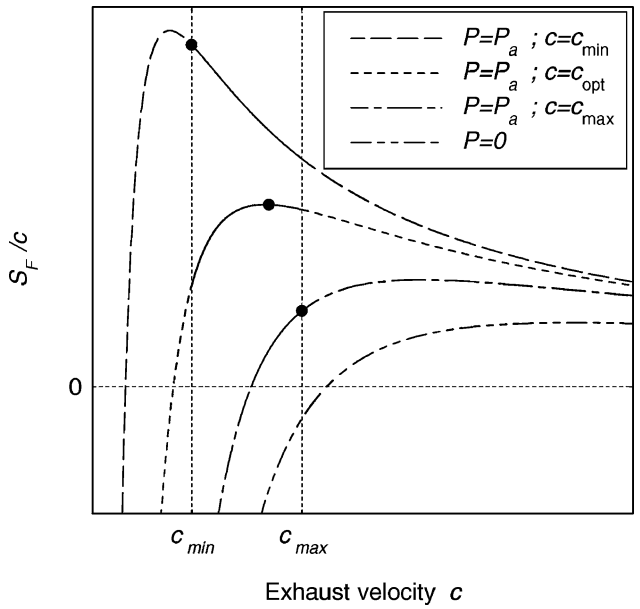

Fig. 1 Selection of the optimal controls for trajectories with bounded-variable I_{sp}.

As far as the selection of the exhaust velocity for a variable-I_{sp} trajectory is concerned, the optimal value c_{opt} is obtained by setting the partial derivative of Eq. (12), with respect to c, to zero. One easily obtains

$$c_{opt} = 2(m\lambda_m/\lambda_v) \tag{19}$$

which corresponds to the maximum of H and is used if it is inside the admissible range for the control ($c_{min} \le c_{opt} \le c_{max}$). Otherwise, the nearest extreme is selected, that is, c_{min} is adopted when $c_{opt} \le c_{min}$, whereas c_{max} is used when $c_{opt} \ge c_{max}$. Figure 1 presents a summary of possible cases and control selections. The same result could be obtained by considering $1/c$, which is proportional to the thrust, as the control variable. The Hamiltonian is a quadratic function of $1/c$, and a standard optimization problem arises.

It can easily be seen[11] that $m^2\lambda_m = b$ is constant; in fact, by using Eqs. (3) and (15) one obtains

$$\frac{\mathrm{d}(m^2\lambda_m)}{\mathrm{d}t} = \lambda_v T - 2m\lambda_m \frac{T}{c} \tag{20}$$

which is identically null when the thruster operates with the optimal c provided by Eq. (19). Therefore c_{opt} is inversely proportional to the product of the spacecraft mass and primer vector magnitude: $c_{opt} = 2b/(m\lambda_v)$. It has been shown[7] that, in the absence of losses, c is inversely proportional to m only.

Dual-I_{sp} Thruster

This paper mainly focuses on dual-I_{sp} propulsion. Equation (18) is again used to state when the thruster is turned on or off. The exhaust velocity of the thruster, when it is not switched off, can be either c_{min} or c_{max}. The maximization of the Hamiltonian requires the transition from high to low specific impulse, that is, $c = c_{min}$, when

$$(\lambda_v/m - \lambda_m/c_{min})(1/c_{min}) > (\lambda_v/m - \lambda_m/c_{max})(1/c_{max}) \tag{21}$$

Equation (21) is rearranged in the form

$$\lambda_v/m > \lambda_m(1/c_{min} + 1/c_{max}) \tag{22}$$

The switching function for the exhaust velocity is introduced

$$S_c = \lambda_v/m - \lambda_m(1/c_{min} + 1/c_{max}) \tag{23}$$

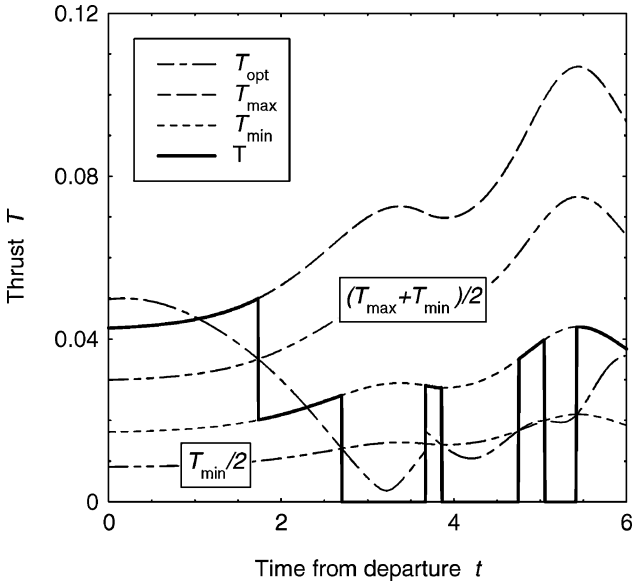

Fig. 2 Selection of the thrust level of a dual-I_{sp} thruster.

and one recognizes that low specific impulse ($c = c_{min}$), that is, high thrust, is used when S_c is positive. An alternative criterion is found by multiplying Eq. (23) by $\eta P/\lambda_m$. One obtains

$$S_c(\eta P/\lambda_m) = (\lambda_v/m)(\eta P/\lambda_m) - \eta P(1/c_{min} + 1/c_{max}) \tag{24}$$

and, using Eqs. (9) and (19),

$$S_c(\eta P/\lambda_m) = T_{opt} - (T_{max} + T_{min})/2 \tag{25}$$

where $T_{opt} = 2\eta P/c_{opt}$ is the optimal thrust value for an engine with unbounded variable I_{sp}. Then, $S_c > 0$ implies

$$T_{opt} > (T_{max} + T_{min})/2 \tag{26}$$

The preceding analysis can be applied to an engine that can switch between any number of discrete values of the specific impulse c_j, each generating the thrust $T_j = 2\eta P/c_j$. A meaningful criterion to switch from T_{j-1} to the adjacent higher thrust level T_j is

$$T_{opt} > (T_j + T_{j-1})/2 \tag{27}$$

One should select the exhaust velocity that produces the thrust which is closer to T_{opt}. Equation (27) is valid between two adjacent values of thrust, including the zero-thrust (i.e., power-off) level. Figure 2 describes the application of the aforementioned criterion during the first phase of a Mercury mission with a Venus flyby. The thruster is switched from $T = 0$ to $T = T_{min}$ when $T_{opt} > T_{min}/2$, and vice versa. The switch from $T = T_{min}$ to $T = T_{max}$ occurs when $T_{opt} > (T_{min} + T_{max})/2$. The available thrust varies as a result of the continuously varying distance from the sun. One should note that T_{opt} is discontinuous in correspondence of the flyby.

The same procedure, which is used for a constant-I_{sp} operation, is adopted to select the most suitable values of the exhaust velocity of the dual-I_{sp} thruster. Each level of exhaust velocity (c_{min}, c_{max}) is considered as an additional (constant) state variable. Two adjoint variables λ_c are added, and the integration of the corresponding Euler–Lagrange equation, that is, Eq. (17), is carried out only when the relevant exhaust velocity is selected. The boundary conditions state the nullity of both the adjoint variables at t_0 and t_f.

Boundary Conditions for Optimality

The boundary conditions for optimality do not differ from the constant-I_{sp} case[12,13] and are only summarized here. When the area of the solar-array surface, and the corresponding electric power, are assigned, the search for the maximum payload is equivalent to maximizing the spacecraft mass m_f at the end of the mission.

The adjoint variables are free at the initial and final points, but $\lambda_{mf} = 1$. This condition is however replaced by $\lambda_{m0} = 1$ because the problem is homogeneous in the adjoint variables. The transversality condition provides $H'_0 = H'_f$, which, with the addition of the trip time constraint, implicitly determines departure and arrival times. In the absence of such a constraint, $H'_f = 0$ should instead be enforced; however, the trip time would grow to infinity, as the thruster would operate with infinite specific impulse and infinitesimal thrust. A previous article[11] presents the boundary conditions for an optimal flyby.

The optimization procedure can also provide the value of the nominal thrust power P_1 that maximizes the payload $m_u = m_f - \alpha P_1/\eta = m_f - \beta P_1$, where α is the specific mass of the power generator and η the thruster efficiency. The constant state variable P_1 and the adjoint variable λ_P are added, and the Euler–Lagrange equation during a thrust arc

$$\frac{\mathrm{d}\lambda_P}{\mathrm{d}t} = -\frac{\partial H}{\partial P_1} = -\frac{H'}{P_1} \tag{28}$$

is obtained from Eq. (11) using Eq. (12) because a bang-bang control is optimal for the power level and P is therefore directly proportional to P_1. Equation (28) is integrated when the thruster is on, whereas λ_P is constant during a coast arc ($H' = 0$); the boundary conditions for optimality prescribe[11] $\lambda_{P0} = 0$ and $\lambda_{Pf} + \beta\lambda_{mf} = 0$. The optimal unconstrained-I_{sp} solution implies[11] $m_u = m_f^2$; this relation seems to have a more general validity.[7]

Numerical Results

The boundary-value problem, which arises from the application of the theory of optimal control, is solved by a procedure,[16] which is based on Newton's method. To obtain a more precise integration and easier convergence, the trajectory is split into arcs with homogeneous control laws. The continuity of H is enforced by setting the relevant switching function to zero at the arc junctions, where the exhaust velocity and/or the thrust undergo a jump, implicitly determining the switching times.

Missions to Venus and Mars are first considered to evaluate the characteristics and the benefits of using variable-specific-impulse compared to the constant-I_{sp} case. A coefficient $\beta = \alpha/\eta = 10$, which corresponds to $\alpha = 40$ kg/kW for a thruster with $\eta = 0.7$, has been assumed to account for the generator mass and evaluate the payload. To obtain more general results, the position of the arrival planet is left free, that is, the spacecraft is inserted into the same orbit of the planet around the sun, but the target planet is in a different position.[12] Thus, mission performance is not affected by the phase angle between the Earth and the target planet. The imposed boundary conditions at the final point can be found elsewhere.[12]

More realistic missions aimed at Mercury have also been considered, taking the actual positions of the planets into account. These missions experience a large benefit in delivered payload from the management of the available power, which exhibits a 10-fold variation caused by the vehicle's varying distance from the sun. The optimal specific impulse presents a very large variation along the trajectory, and a suitable thruster will not be available in the near term. Therefore, the analysis has been extended to bounded-I_{sp} and dual-I_{sp} thrusters. The performance of a rendezvous mission is strongly related to the phase angle between the relevant planets. To avoid additional complexity during the discussion of the results, the area of the solar-array surface has not been optimized, that is, the nominal available power is the same for all of the Mercury missions.

Venus and Mars Missions

Missions to Venus are considered in Figs. 3 and 4. Figure 3 compares variable-I_{sp} and constant-I_{sp} trajectories in terms of payload and average exhaust velocity $c_{avg} = g_0(I_{sp})_{avg}$, where the average specific impulse is computed as the ratio of the total impulse to the consumed propellant. The trip time has been fixed at either $\tau = 8$ or 12 (about 465 or 698 days, respectively). Figure 4 shows the control and thrust histories for missions with $\eta P_1 = 0.01$ and $\tau = 8$.

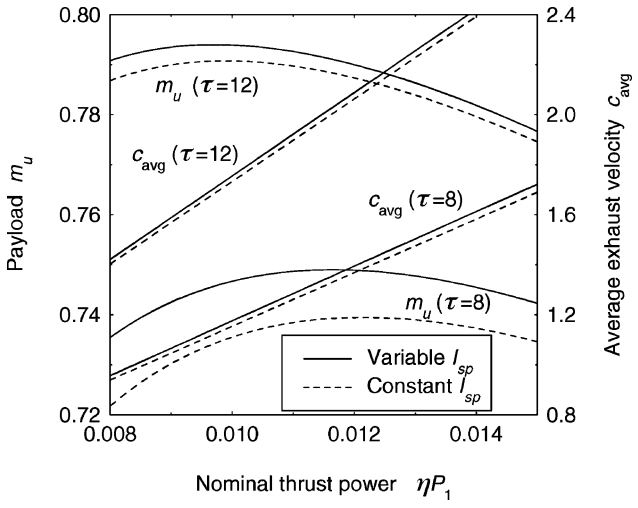

Fig. 3 Performance comparison of direct missions to Venus ($\tau = 8$ and 12).

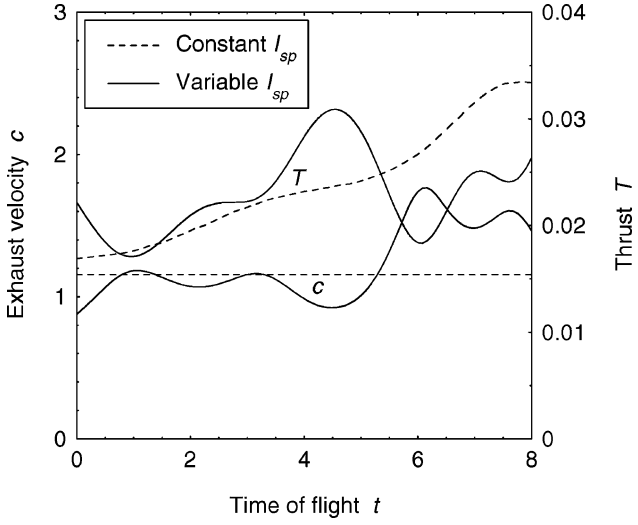

Fig. 4 Control law for direct missions to Venus ($\eta P_1 = 0.01$, and $\tau = 8$).

It is well known that an optimal value of the thrust power exists for each trip time. The performance improves for the same value of the available power as the mission trip time grows because the same total impulse can be provided with lower thrust and, conversely, with higher specific impulse and lower propellant consumption. The payload can be further increased by reducing the power and the corresponding generator mass; the related payload benefit overcomes the penalty caused by the specific-impulse reduction. (In Fig. 3, the position of the maximum payload shifts to the left when τ grows, and the optimal power is lower in the case of variable specific impulse.)

The most important feature, which is highlighted in Fig. 3, is that the payload benefit of variable-I_{sp} trajectories over constant-I_{sp} trajectories is significant especially if the trip time is short. In this case the increased control capability allows the mission designer to obtain a larger payload by reducing the losses that are related to the magnitude and direction of the thrust, whereas the average specific impulse is almost the same for constant and variable-I_{sp} thrusters. For instance, the specific impulse is reduced and higher thrust can be used where it is more beneficial for the reduction of gravitational losses. Figure 4 shows that the larger power that is available in the last phase of a mission to an inner planet is used to increase the specific impulse, according to simpler theoretical analyses,[6,7] whereas the thrust level is almost constant.

Missions to Mars present similar features. However, the spacecraft moves toward an outer planet, and, during the variable-I_{sp} operation, the reduction of the available power mainly affects the

thrust level, whereas the exhaust velocity is kept almost constant, as shown in Fig. 5, which presents the control history for missions with $\eta P_1 = 0.01$ and $\tau = 10$. The average specific impulse is however larger for the variable-I_{sp} thruster, which can compensate for the lower average thrust by properly throttling the engine, when required.

Mercury Missions

The procedure presented in this paper has then been applied to analyze actual rendezvous missions to Mercury, flying either a direct or a Venus-gravity-assist (VGA) trajectory. Venus is in a favorable position for a flyby in 2006, and departure in 2005 has therefore been selected. Because the absolute positions of the Earth and Venus repeat almost exactly every eight years, similar VGA missions can be flown departing in 2013. Direct trajectories can instead be flown every year with almost identical performance. The nominal available power is not optimized, and the same area of the solar-array surface is assumed throughout. The required data are only the planets' ephemerides and the maximum beam power at 1 AU; the assumed value is $\eta P_1 = 0.02$.

Table 1 presents the main characteristics of direct missions with assigned trip time varying between 10 and 15 (581 and 872 days, respectively). Table 2 presents the same characteristics for VGA trajectories. The optimal values of the specific impulse have been adopted for constant-I_{sp} and dual-I_{sp} trajectories. The values of the latter class of missions have been assumed as c_{min} and c_{max} for the corresponding bounded-I_{sp} trajectories. The final mass is increased by the gravity assist from Venus, by selecting a thruster with increased control capabilities, or by allowing a longer trip time, which permits the use of reduced thrust levels and larger values of specific impulse.

Table 1 Performance comparison: direct missions to Mercury ($\eta P_1 = 0.02$)

	Trip time τ		
Mission characteristics	10	12.5	15
Constant I_{sp}			
m_f	0.5999	0.6513	0.6959
c	1.2954	1.5611	1.8626
Dual I_{sp}			
m_f	0.6303	0.6785	0.7137
c_{min}	0.8780	1.1701	1.4133
c_{max}	1.7106	2.0833	2.4670
c_{avg}	1.3689	1.6484	1.9159
Bounded I_{sp}			
m_f	0.6333	0.6816	0.7167
Variable I_{sp} (unbounded)			
m_f	0.6365	0.6843	0.7210
c_{avg}	1.3920	1.6793	1.9462

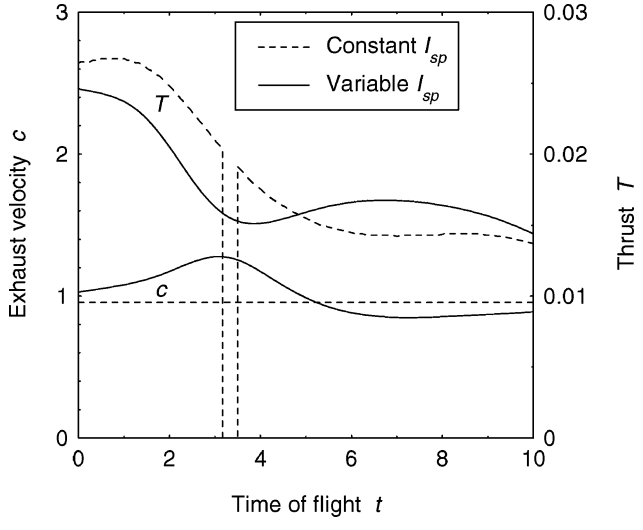

Fig. 5 Control law for direct missions to Mars ($\eta P_1 = 0.01$, and $\tau = 10$).

Table 2 Performance comparison: VGA missions to Mercury ($\eta P_1 = 0.02$)

	Trip time τ		
Mission characteristics	10	12.5	15
Constant I_{sp}			
m_f	0.7212	0.7609	0.7856
c	1.5720	1.7248	1.8881
Dual I_{sp}			
m_f	0.7447	0.7717	0.8178
c_{min}	1.3556	0.9260	1.2845
c_{max}	2.1124	2.3017	3.1690
c_{avg}	1.6873	1.7943	2.4309
Bounded I_{sp}			
m_f	0.7460	0.7741	0.8193
Variable I_{sp} (unbounded)			
m_f	0.7489	0.7831	0.8227
c_{avg}	1.6901	1.9085	2.4160

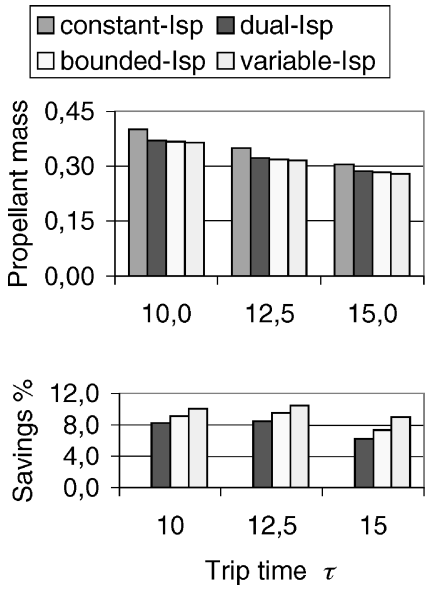

Fig. 6 Propellant consumption for direct missions to Mercury ($\eta P_1 = 0.02$).

The same missions that are shown in Tables 1 and 2 are compared, in terms of propellant consumption, in Figs. 6 and 7, which also show that the variable-I_{sp} thruster permits a 10% mean reduction in the propellant consumption. This value doubles in special cases (i.e., long missions with Venus gravity assist), when the propellant mass is very low. Most of the benefit (roughly 80%) could be obtained using a dual-mode thruster, which appears to be even more competitive when one considers that upper and lower limits for the specific impulse are unavoidable, at least in the short term.

Actual mission opportunities have been considered, and the presence of apparently anomalous results is caused by the presence of time constraints and the necessity of taking the planets' phase angles into account. In some instances, mission performance is greatly affected and penalized. The VGA missions with $\tau = 12.5$ are emblematic of this occurrence. Figure 8 presents the dual-I_{sp} VGA trajectory, which reaches Mercury with this particular value of the trip time. Coast arcs are present, and the values of c are lower than expected (see Table 2) because a large thrust is necessary to intercept the planets. The optimal control law of this mission is compared in Fig. 9 with the control law of the unbounded variable-I_{sp} case, with the same trip time. Figure 10 presents the same comparison for longer missions ($\tau = 15$), which are characterized by quite different control histories, compared to the shorter missions. The position of Venus at the flyby, that is, the flyby date, is practically

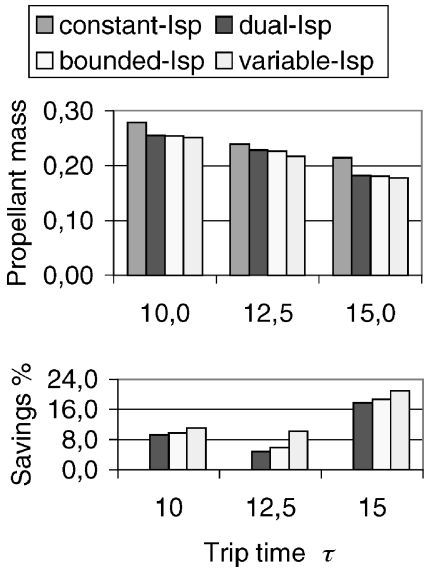

Fig. 7 Propellant consumption for VGA missions to Mercury ($\eta P_1 = 0.02$).

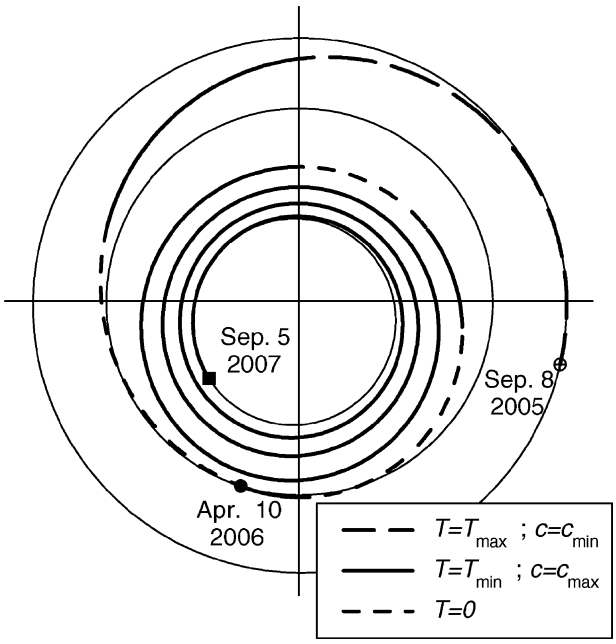

Fig. 8 Dual-I_{sp} VGA mission to Mercury ($\eta P_1 = 0.02$, and $\tau = 12.5$).

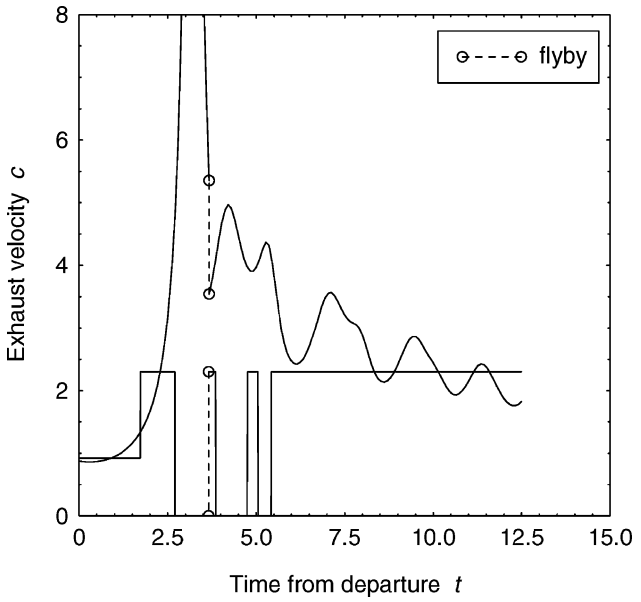

Fig. 9 Control law for VGA missions to Mercury ($\eta P_1 = 0.02$, and $\tau = 12.5$).

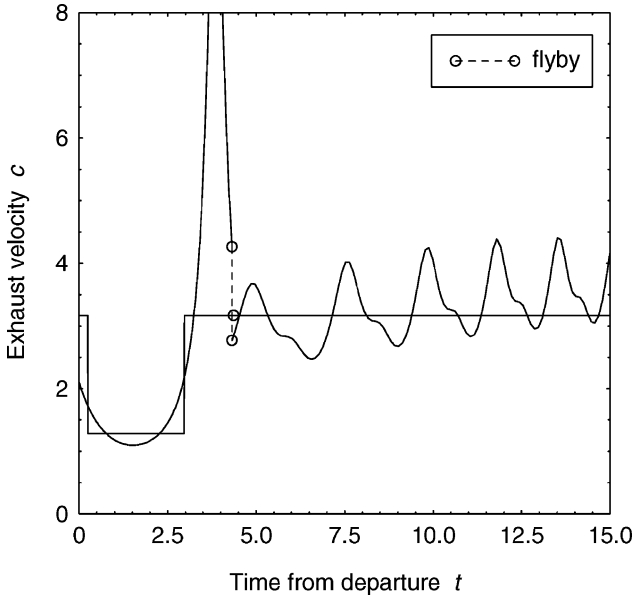

Fig. 10 Control law for VGA missions to Mercury ($\eta P_1 = 0.02$, and $\tau = 15$).

fixed, because of the necessity of obtaining a free rotation of the trajectory plane. When Mercury is not correctly phased to Venus (as for $\tau = 12.5$), a small portion of the available time is subtracted from the Earth–Venus leg and transferred to the Venus–Mercury leg, which also requires a larger thrust to compensate for the unfavorable phase angle. Soon after the late departure, the shorter missions require higher thrust to reach Venus with a faster trip. Moreover, the increased available power near Mercury is used mainly to obtain the required high thrust, while the exhaust velocity is progressively reduced. On the contrary, Mercury is in a favorable position with respect to Venus when $\tau = 15$, and the specific impulse can be gradually increased, as is suggested by quite general criteria concerning the management of the available energy.[7] The initial requirement of higher thrust, which is necessary in the case of the shorter missions, could be replaced by a nonzero hyperbolic excess velocity at departure, that is, by the contribution of the chemical motor used to leave the low Earth orbit. This consideration, which has already been included in the optimization procedure,[17] could relieve the difficulties that are specific to the faster VGA missions.

Conclusions

It is well known that a thruster with variable specific impulse could significantly improve the performance of a spacecraft that uses the same electric engine to escape from the Earth and to maneuver in deep space. The present analysis has shown that a similar engine, with a limited range of specific impulse, is also useful when it is used only during the interplanetary portion of the trajectory. The additional control capability that is available during a variable-I_{sp} trajectory, compared to a constant-I_{sp} trajectory, reduces the propellant consumption. General considerations suggest to privilege the use of high specific impulse with respect to the thrust level, as the propellant is gradually consumed. Occasionally, a higher thrust can be made available when it is necessary to reduce the losses that are caused by the finite thrust level, thus overcoming the penalty caused by a lower specific impulse. Moreover, better management of the electric power allows the mission designer to select a lower level of nominal power, and the reduced mass of the power generator results in an extra benefit in terms of payload. Numerical results show that

most of the benefit is obtained when the engine can simply operate with two different values of the specific impulse, without the requirements of a thruster that is continuously throttled. This kind of thruster can be more easily developed and made available sooner than the continuously throttled thruster.

References

[1]Ho, D. Y., "The Year in Review: Electric Propulsion," *Aerospace America*, Vol. 39, No. 12, 2001, p. 58.

[2]Patterson, M. J., Haag, T. W., Foster, J. E., Rawlin, V. K., Roman, R. F., and Soulas, G. C., "Development Status of a 5/10-kW Class Ion Engine," AIAA Paper 2001-3489, July 2001.

[3]Killinger, R., Bassner, H., Mueller, J., Kukies, R., and Leiter, H. J., "High Performance RF-Ion Thruster Development (RIT XT)—Performance and Durability Test Results," AIAA Paper 2001-3488, July 2001.

[4]King, D. Q., de Grys, K. H., and Jankovsky, R., "Multi-Mode Hall Thruster Development," AIAA Paper 2001-3778, July 2001.

[5]Chand Diaz, F. R., Squire, J. P., Bengston, R. D., Breizman, B. N., Baity, F. W., and Carter, M. D., "The Physics and Engineering of the Vasimr Engine," AIAA Paper 2000-3756, July 2000.

[6]Bishop, R. H., and Azimov, D. M., "Analytical Space Trajectories for External Motion with Low-Thrust Exhaust-Modulated Propulsion," *Journal of Spacecraft and Rockets*, Vol. 38, No. 6, 2001, pp. 897–903.

[7]Colasurdo, G., and Casalino, L., "Energy Management in Rocket Propulsion," *Journal of Propulsion and Power*, Vol. 16, No. 4, 2000, pp. 705–708.

[8]Prussing, J. E., "Equation for Optimal Power-Limited Spacecraft Trajectories," *Journal of Guidance, Control, and Dynamics*, Vol. 16, No. 2, 1993, pp. 391–393.

[9]Kechichian, J. A., "Optimal Low-Thrust Transfer Using Variable Bounded Thrust," *Acta Astronautica*, Vol. 36, No. 7, 1995, pp. 357–365.

[10]Lawden, D. F., *Optimal Trajectories for Space Navigation*, Butterworths, London, 1963, pp. 54–68.

[11]Casalino, L., Colasurdo, G., and Pastrone, D., "Optimal Low-Thrust Escape Trajectories Using Gravity Assist," *Journal of Guidance, Control, and Dynamics*, Vol. 22, No. 5, 1999, pp. 637–642.

[12]Colasurdo, G., and Casalino, L., "Trajectories Towards Near-Earth Objects Using Solar Electric Propulsion," American Astronautical Society, Paper 99-339, Aug. 1999.

[13]Colasurdo, G., and Casalino, L., "Optimal Time-Constrained Missions to Near-Earth Asteroids," International Astronautical Federation, Paper 01-A-5.04, Oct. 2001.

[14]Hechler, M., "Mercury Orbiter Mission Analysis: On Mission Opportunities with Chemical and Solar Electric Propulsion," MAS WP 389, ESOC, Darmstadt, Germany, Oct. 1996.

[15]Casalino, L., "Singular Arcs During Aerocruise," *Journal of Guidance, Control, and Dynamics*, Vol. 23, No. 1, 2000, pp. 118–123.

[16]Colasurdo, G., and Pastrone, D., "Indirect Optimization Method for Impulsive Transfer," *AIAA/AAS Astrodynamics Conference: A Collection of Technical Papers*, AIAA, Washington, DC, 1994, pp. 441–448.

[17]Casalino, L., Colasurdo, G., and Faga, M., "Indirect Optimization of Multi-Flyby Mercury Rendezvous Missions," International Astronautical Federation, Paper 00-A.4.02, Oct. 2000.